CALCULATING MASS TRANSFER IN ECCENTRIC BINARIES USING THE BINARY EVOLUTION CODE BINSTAR

P. J. Davis[1], L. Siess[1] and R. Deschamps[1]

Abstract. We present calculations of mass transfer via Roche lobe overflow for a $1.50 + 1.40$ M$_\odot$ main sequence binary system with an eccentricity of 0.25 and orbital period of approximately 0.7 d using the state-of-the-art binary evolution code `BINSTAR`. We consider the effect of eccentricity and an asynchronously rotating donor star on the Roche lobe radius, and investigate their impact on the mass transfer rate.

Keywords: Binaries: close, stars: evolution, methods: numerical

1 Introduction

Studies of interacting binaries typically assume that the orbit is circular and that the donor is rotating synchronously with the orbit by the time Roche-lobe overflow (RLOF) commences, as a result of the short timescales over which tidal forces act (Zahn 1977). However, such assumptions have been challenged by observations of ellipsoidal variables with confirmed significant eccentricities (Nicholls & Wood 2012). Furthermore, Sepinsky et al. (2007b, 2009) found that mass transfer via RLOF in eccentric binaries may act to increase the eccentricity on a shorter timescale than the tidal circularization timescale which acts to decrease it.

In an accompanying paper, Sepinsky, Willems, & Kalogera (2007a) found that the Roche lobe radius for a donor star, which is rotating super-synchronously compared with the orbital motion at periastron is smaller than the radius calculated using the standard Eggleton (1983) prescription. These effects, of eccentricity and asynchronism, directly affect the RLOF mass transfer rate, and have been modelled using the state-of-the-art binary evolution code `BINSTAR`.

Here, we consider a 1.50+1.40 M$_\odot$ binary, with an eccentricity of 0.25, and an initial period $P_{\rm orb} \approx 0.7$ d. The impact of asynchronous rotation and eccentricity on the mass transfer rate are investigated, as well as the response of the structure of the donor and accretor. In Sect. 2, we describe the `BINSTAR` code, and the key input physics. Calculated mass transfer rates are presented in Sect. 3, while the reaction of the stars to mass transfer is discussed in Sects. 4 and 5. A summary is given in Sect. 6.

2 Computational method

`BINSTAR` is designed for the evolution of low- and intermediate-mass binaries. It is an extension of the 1-dimensional, single star evolution code `STAREVOL` (see Siess 2010, and references therein). Briefly, `BINSTAR` simultaneously solves for the orbital eccentricity and separation, and the two stars. `BINSTAR` also handles semi-convection, thermohaline mixing and diffusive overshooting and includes a nuclear network of 53 species (up to ^{37}Cl). For further details of the binary input physics, see Siess et al. (2013).

2.1 The initial binary model

We consider a main sequence binary consisting of a donor star of mass $M_{\rm d} = 1.50$ M$_\odot$ with a gainer of mass $M_{\rm g} = 1.40$ M$_\odot$, with radii $R_{\rm d} = 1.44$ R$_\odot$ and $R_{\rm g} = 1.23$ R$_\odot$ respectively. The stars have an age of approximately 1.3 Gyr and a metallicity of $Z = 0.001$, and we use a convection mixing length of $\alpha_{\rm MLT} = 1.71$. We do not consider convective overshooting. The binary has an eccentricity $e = 0.25$ and a semi-major axis $a = 4.80$ R$_\odot$.

---

[1] Institut d'Astronomie et d'Astrophysique, Université Libre de Bruxelles, Boulevard du Triomphe, Brussels 1050, Belgium
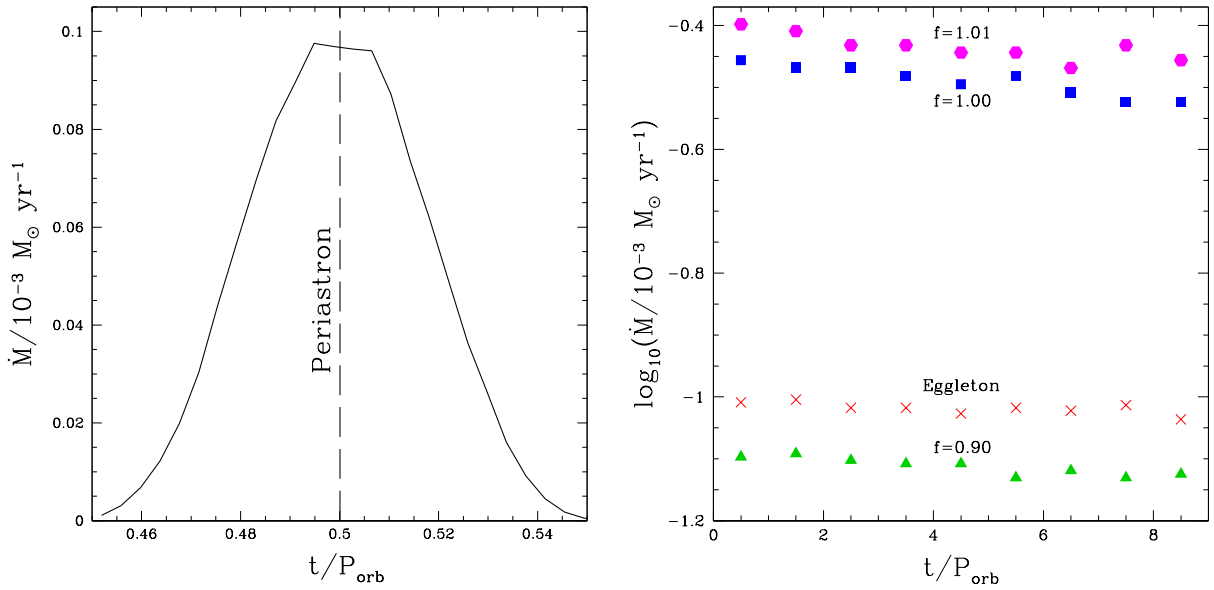
Fig. 1. Left: Mass transfer rate as a function of time since apastron, where time is in units of the orbital period, and the standard Roche formalism is used (Eq. 2.1). The dashed, vertical line indicates periastron. **Right:** Periastron mass transfer rate during 9 consecutive orbits for the standard Roche formalism (red crosses), $f = \Omega/\omega_{\text{peri}} = 0.90$ (green triangles), $f = 1.00$ (blue squares) and $f = 1.01$ (magenta hexagons).

2.2   Roche lobe radius

For an eccentric binary in synchronous rotation where the separation between the two stars is D, the Roche lobe radius of the donor star, $R_{\mathcal{L}_1}$, is

$$R_{\mathcal{L}_1} = \frac{0.49q^{2/3}}{0.6q^{2/3} + \ln(1 + q^{1/3})}D, \qquad (2.1)$$

where $q = M_{\text{d}}/M_{\text{g}}$ and we have modified the expression for $R_{\mathcal{L}_1}$ given by Eggleton (1983) by replacing a with D. For brevity, we henceforth term this as the 'standard Roche formalism'.

We also follow Sepinsky et al. (2007a) and calculate $R_{\mathcal{L}_1}$ by taking into account the eccentricity of the orbit, and any asynchronism of the donor star. The potential in this case (normalized to the gravitational potential of the accretor), is given by

$$\Psi = -\frac{q}{(x^2 + y^2 + z^2)^{\frac{1}{2}}} - \frac{1}{[(x - 1)^2 + y^2 + z^2]^{\frac{1}{2}}} - \frac{1}{2}\frac{f^2(1 + e)^4}{(1 + e \cos \nu)^3}(1 + q)(x^2 + y^2) + x, \qquad (2.2)$$

where the x-axis lies along the line joining the centers of mass of the two stars, in the direction from the donor to the accretor, the z-axis is perpendicular to the plane of the orbit and is parallel to the spin angular velocity vector of the donor, and the y-axis is perpendicular to the x- and z-axes, and completes a right-handed coordinate set. All coordinates are given in units of D. We use a Monte-Carlo integration technique to calculate $R_{\mathcal{L}_1}$ from Eq. (2.2). In Eq. (2.2) f is the spin angular speed of the donor star in units of the orbital angular speed at periastron, i.e.

$$f = \frac{\Omega}{\omega_{\text{peri}}}. \qquad (2.3)$$

2.3   Calculating mass transfer rates

We consider a donor star of mass M_{d}, radius R_{d}, effective temperature $T_{\text{eff,d}}$, and with a mean molecular weight and density at the photosphere, $\mu_{\text{ph,d}}$ and $\rho_{\text{ph,d}}$ respectively. The mass transfer rate, $\dot{M}_{\text{d}}$, in the case where

material is removed from the optically thin region of the donor's atmosphere (i.e. where the optical depth is $\tau \leq \frac{2}{3}$) is calculated using

$$- \dot{M}_{\rm d} = \dot{M}_0 \exp\left(\frac{R_{\rm d} - R_{\mathcal{L}_1}}{\hat{H}_{\rm P}}\right), \tag{2.4}$$

(Ritter 1988) where $\hat{H}_{\rm P}$ is the pressure scale height of the donor at the location of the inner Lagrangian point $\mathcal{L}_1$, and $\dot{M}_0$ is the mass transfer rate if the donor star exactly fills its Roche lobe. Equation. (2.4) is only valid if the donor star is slightly over- or under-filling its Roche lobe. If this is not the case, then mass is also lost from the optically thick layers of the star (where $\tau \geq 2/3$). The mass transfer rate is therefore given by

$$- \dot{M}_{\rm d} = \dot{M}_0 + 2\pi F(q) \frac{R_{\mathcal{L}_1}^3}{GM_{\rm d}} \int_{R_{\mathcal{L}_1}}^{R_{\rm ph}} \Theta(\Gamma_1) \frac{Gm(P\rho)^{\frac{1}{2}}}{r^2} \, {\rm d}r, \tag{2.5}$$

(Kolb & Ritter 1990) where $F(q)$ is determined from the area of the equipotential surface which intersects with the $\mathcal{L}_1$ point. Also, P, T, μ and m are the pressure, temperature, mean molecular weight and the mass of the donor star respectively at the radial coordinate r. Next, $\Theta(\Gamma_1)$ is a function of the adiabatic exponent, $\Gamma_1 = ({\rm dln}P/{\rm dln}\rho)_{\rm ad}$ (see Kolb & Ritter 1991 for further details). The integral in Eq. (2.5) is evaluated numerically from the $\mathcal{L}_1$ point to the photosphere (subscript 'ph').

3   Calculated mass transfer rates

The left panel of Fig. 1 shows that $|\dot{M}_{\rm d}|$ rises as the stars approach periastron (dashed vertical line), reaching about 10^{-4} M$_\odot$ yr^{-1} for the standard Roche formalism. This behaviour is due to the fact that $R_{\mathcal{L}_1}$ decreases as D decreases (Eq. 2.1) causing a corresponding rise in the amount that the star overfills its Roche lobe, $R_{\rm d} - R_{\mathcal{L}_1}$, and therefore in $|\dot{M}_{\rm d}|$ (Eqs. 2.4 and 2.5). At periastron, $R_{\rm d} - R_{\mathcal{L}_1}$ is maximum. Away from periastron, $R_{\mathcal{L}_1}$ and $R_{\rm d} - R_{\mathcal{L}_1}$ decline causing a drop in $|\dot{M}_{\rm d}|$.

The right panel of Fig. 1 shows that $|\dot{M}_{\rm d}|$ at a given periastron passage increases as f is increased. Indeed, $|\dot{M}_{\rm d}|$ increases from approximately 7×10^{-5} M$_\odot$ yr^{-1} for the sub-synchronous ($f = 0.90$) case to about 4×10^{-4} M$_\odot$ yr^{-1} for the super-synchronous case ($f = 1.01$). If f is increased (causing a corresponding increase in the centrifugal acceleration), then the location of $\mathcal{L}_1$ must be situated closer to the donor star so that a net zero-acceleration is re-established. Since the Roche equipotential surface passes through the $\mathcal{L}_1$ point, an increasing value of f means that both the volume and $\mathcal{L}_1$ will shrink.

4   Reaction of the donor

The inset in Fig. 2 shows that the donor's surface luminosity, $L_{\rm d}$, initially rises at the start of mass loss, due to its small surface convection zone. Mass loss from this layer releases gravo-thermal energy causing $L_{\rm d}$ to briefly increase. However, subsequent reaction is dominated by the extended radiative envelope of the donor. The action of removing mass from the radiative layers absorbs gravo-thermal energy, causing them to be under-luminous compared to an unperturbed star of the same mass. Hence, $L_{\rm d}$ decreases, and the energy deficit within the surface layers causes them to contract (Fig. 2).

Once mass transfer shuts off, the donor radius, $R_{\rm d}$ and $L_{\rm d}$ rise again as energy flows from the donor's interior to fill the luminosity deficit in the outer surface layers as it restores thermal equilibrium. However, the donor does not fully re-establish thermal equilibrium by the time mass transfer resumes at the next periastron passage; the donor is still under-sized and under-luminous (main panel of Fig. 2). As $R_{\rm d}$ shrinks, $R_{\rm d} - R_{\mathcal{L}_1}$ becomes smaller with each successive periastron passage, and the mass transfer rate during periastron will decrease with time. This can be seen in the right panel of Fig. 1.

5   Reaction of the accretor

Towards periastron and in contrast to the donor star, the accretor's surface convection zone continues to play a role in response to mass addition. Mass accretion causes the gainer's surface convection zone to grow in size (see Davis, Siess, & Deschamps 2013, for details), and subsequent addition of mass to the convection zone absorbs gravo-thermal energy. These layers become under-luminous (inset of Fig. 2) and as a result, they contract.

Beyond periastron, with the decline in $|\dot{M}_{\rm d}|$, the surface layers re-expand and the luminosity increases as energy from the accretor's interior flows outwards to the under-luminous layers. Once mass transfer shuts off,
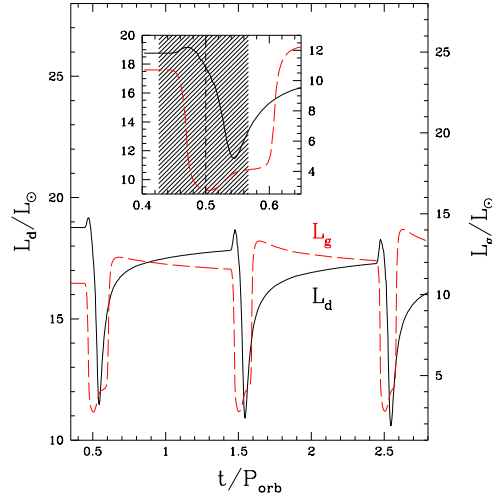
Fig. 2. Time evolution of the donor's luminosity, L_d (left axis, solid black curve), and accretor's luminosity, L_g (right axis, dashed red curve), during mass transfer using the standard Roche formalism. The inset shows a close-up of the first periastron passage. The shaded region gives the duration of mass loss, while the dotted vertical line indicates periastron.

the expansion of the surface layers continue. However, once the excess energy originally created by the accretion phase has been radiated away, both the radius and surface luminosity start to slowly decrease.

6   Summary

We present the first calculations of mass transfer in an eccentric binary system using a detailed stellar and binary evolution code, called BINSTAR. The evolution of the mass transfer rate has a Gaussian-like profile, with mass transfer commencing (ending) just before (after) periastron, in agreement with recent smooth particle hydrodynamical simulations (Lajoie & Sills 2011; Davis et al. 2013). The mass transfer rate is maximum at periastron, and using the standard Eggleton (1983) formalism it peaks at about 10^{-4} $M_\odot$ yr^{-1}. This is about a factor of 3 smaller than the synchronous $f = 1.00$ case (which includes the effects of eccentricity), highlighting the need to account for the non-circular nature of the orbit when determining the Roche lobe radius. During mass transfer, the donor's radius and luminosity decline due to its substantial radiative envelope. As a result of the accretor's growing surface convection zone during accretion, its radius and surface luminosity initially shrink until periastron, after which they rise. Both stars do not fully re-establish thermal equilibrium by the time mass transfer re-commences.

References

Davis, P. J., Siess, L., & Deschamps, R. 2013, A&A (submitted)

Eggleton, P. P. 1983, ApJ, 268, 368

Kolb, U. & Ritter, H. 1990, A&A, 236, 385

Lajoie, C.-P. & Sills, A. 2011, ApJ, 726, 67

Nicholls, C. P. & Wood, P. R. 2012, MNRAS, 421, 2616

Ritter, H. 1988, A&A, 202, 93

Sepinsky, J. F., Willems, B., & Kalogera, V. 2007a, ApJ, 660, 1624

Sepinsky, J. F., Willems, B., Kalogera, V., & Rasio, F. A. 2007b, ApJ, 667, 1170

Sepinsky, J. F., Willems, B., Kalogera, V., & Rasio, F. A. 2009, ApJ, 702, 1387

Siess, L. 2010, A&A, 512, A10

Siess, L., Izzard, R. G., Davis, P. J., & Deschamps, R. 2013, A&A (submitted)

Zahn, J.-P. 1977, A&A, 57, 383